Natural Hazards
and Earth System
Sciences

Open Access

Discussions

EGU

Assessing the tsunami building vulnerability PTVA-3 and PTVA-4 models after the 16S 2015 event in the cities of Coquimbo – La Serena (Chile)

Eduardo Fritis[1], Tatiana Izquierdo[1], Manuel Abad[1]

5   [1]Departamento de Geología, Universidad de Atacama, Avenida Copayapu 485, Copiapó, Chile

Correspondence to: Tatiana Izquierdo (tatiana.izquierdo@uda.cl)

Abstract. Chile is highly exposed to tsunamigenic events, as the one occurred in September 16, 2015; however, it has not been until recent years that land-use policies have begun to be considered. These new regulations must identify the most vulnerable sectors of the Chilean coastal cities. This paper analyses and validates the use of the two latest versions of the

10   PTVA model in the 2015 tsunami scenario in the cities of La Serena and Coquimbo and their potential use in other Chilean cities in future land-use or mitigation measures planning. Both models result in a similar number of very-high and high RVI scores. However, the less vulnerable categories do not show a similar trend and the PTVA-4 model obtains a larger number of minor and average RVI scores. When compare with the damages caused by the tsunami, the PTVA-3 show a more similar distribution to the actual damages than that obtained by the PTVA-4 model that shows a more concentrated distribution of

15   the RVI scores.

1 Introduction

Tsunamigenic events in Chile are a consequence of the convergence boundary in which the Nazca plate subducts under the South American plate at a rate of 74 mm/yr (DeMets et al., 2010). In fact, three of the last eight largest earthquakes (Mw> 8) occurred during the last six years around the world have occurred in Chile: Maule 2010, Mw=8.8; Iquique 2014, Mw=8.2;

20   and Illapel 2015 Mw= 8.4. All of them were tsunamigenic. The first historical observations of earthquakes and tsunamis in the Pacific coast of South America date from the 16th century with the arrival of the Spaniards to this region, although there are more ancient descriptions of these catastrophes in Peruvian and Chilean legends (Kulikov et al., 2005). Especially relevant was the earthquake occurred on May 22, 1960 (Mw~9.5) with a rupture zone of almost 1,000 km (Smith, 2010) that triggered a tsunami that affected the entire Chilean coast as well as Hawaii, Japan, the Philippines, New Zealand, Australia

25   and Alaska (SHOA, 2000). Likewise, tsunamigenic earthquakes that occur in other subduction zones of the Pacific Ocean can affect the Chilean coast. The most recent example is the earthquake that occurred on March 11, 2011 in Tōhoku, Japan (Mw = 9.0; Simons et al., 2011) that arrived at the Chilean coasts after 21 hours (Dunbar et al., 2011) with a maximum observed amplitude of 2.23 m in Arica and Talcahuano cities (SHOA, 2016).

The historical record includes dozens of destructive tsunamis on the Chilean coast while the geological record confirms its

30   recurrence in the last thousands of years (Cisternas et al., 2005; Ely et al., 2014; Cisternas et al., 2017; Kempf et al., 2017). In the Coquimbo Region one of the worst tsunamis recorded occurred after the Vallenar earthquake of November 11, 1922 with Mw~8.3. The deformation in the ocean floor triggered a wave train that reached a height of 7 m on the coast of the epicentral region (Caldera-Coquimbo), and the cities of La Serena and Coquimbo were significantly damaged (Beck et al., 1998). According to Bobillier (1926), the tsunami flooded Coquimbo with three waves, the third of which reached an

35   elevation 4.6 m a.s.l. However, Beck et al. (1998) and Lomnitz (2004) refer to a 7m tsunami in the same area. Some zones reached 3 m water depth and horizontal inundation distances of up to 800 m (Contreras-López et al., 2016). In the same context, the water penetrated 2 km at the most low-lying places, and as a result, part of the city situated at the southern apex

of the Coquimbo Bay was completely destroyed, not only by the water, but also by boats and other objects washed ashore (Soloviev and Go, 1975).

Although Chile is highly exposed to these high-energy marine events, it has not been until recent years that land-use planning has begun to be considered. Despite an incipient development of national urban policies is observed after the February 27, 2010 tsunami (Lunecke, 2016), tsunami impact remains a cause for economic and life losses. Among the main advances in land-use planning the Chilean Ministry of Housing and Urban Planning (MINVU) has started to define tsunami hazards areas and, in addition, the National Emergency Office (ONEMI) has included civil protection plans for tsunamigenic events. However, to minimize the losses associated with future tsunamis, it is necessary to assess buildings vulnerability from what is estimated the probable maximum loss (Dall'Osso et al., 2009a). Recently, Aránguiz et al. (under review) have developed fragility curves to assess tsunami damage in Coquimbo after the 2015 tsunami. This method can serve as an adjunct to the PTVA models, like a macro level identification in the assessment tsunami damage builds because offers a binary classification ("low" or "high"). However, it does not include structural details or engineering factors, which are variable in each building. On the other hand, PVTA models include a wider range of variables in the vulnerability assessment. This work evaluates the vulnerability to the tsunami impact for the La Serena-Coquimbo conurbation in the scenario occurred on September 16, 2015 after the tsunami generated by the Illapel earthquake (Mw 8.4). The tsunami had a maximum wave height of 4.7 m in Coquimbo (SHOA, 2016) and caused 11 fatalities (CCT-ONEMI, 2015). For that, we first reconstruct the flood in the cities after inundation heights measured in the field and then, we estimate the Relative Vulnerability Index (RVI) using the PTVA-3 (Dall'Osso et al., 2009a) and PTVA-4 (Dall'Osso et al., 2016) models. Finally, we validate our results by comparing them with the real damages the constructions suffered after the event evaluated by MINVU. This exercise allows us establishing which model can be considered a better approach for tsunami building vulnerability assessment based on the real damages reported after a high-energy marine event.

2 Study area

The cities of La Serena and Coquimbo (412,586 inhabitants) are located in the Coquimbo Region (North-Central Chile), in the so-called "Norte Chico" (Fig. 1). The distance between the oceanic trench and the coast here varies between 80 and 100 km, i.e. it is smaller than in other regions of Chile, where the most typical distances range between 120 and 140 km (Fuentes et al., 2016). According to Tassara et al. (2006) and Pardo et al. (2002) in this zone the subduction angle of the Nazca plate is almost horizontal at depths close to 100 km. This almost horizontal geometry of the plate gives rise to a strongly coupled inter-plate contact, a highly compressed continental crust with back-arc seismicity and shortening of the crust, together with the absence of active quaternary volcanoes in the Andes Cordillera (Jordan et al., 1983).

The Coquimbo Bay is open to the Northwest providing natural protection against the dominant southwestern swells. The submarine part of the bay shows a wide marine platform, close to 10 km, with gentle slope on the seabed. In particular, the Coquimbo Bay exposes depths that do not exceed 50 m inside the bay (Aránguiz et al., 2016). It presents a gentle topography and a more than 110 km long sandy beach only interrupted by the mouth areas of the Culebrón stream and Elqui River which are characterized by the existence of marshlands, much larger in the first case. This marsh parallel to the coast behind the foredune is currently largely anthropized and a high percentage of its original surface is now part of the urban area (Fig. 1).

In the Coquimbo - La Serena conurbation, the urbanization process and the coastal border occupation have caused a convergence in the coastal space of several uses causing conflicts (Hidalgo et al., 2009). At present, due to rapid growth and discrepancies in the coastal sector regulations (Maureira, 1998) several uses appear in the littoral such as residential, commercial, industrial and tourist as well as illegal settlements, what results in different construction types. In addition, there is no capacity for a complete evacuation of the coastal border in case of a tsunami especially during the summer season due to the high number of tourist (McBride et al., 2016).

3 Methodology

3.1 GIS Geodatabase

We developed a Geographic Information System (GIS) based geodatabase that gathers different spatial information needed for the vulnerability calculation. On the one hand, the city cartography was downloaded from the Copernicus Emergency

5 Management Service of the European Union webpage (http://emergency.copernicus.eu) whereas the tsunami flood scenario was reconstructed after a field survey (see section 3.2).

3.2 Tsunami inundation map

To reconstruct the flood scenario a field survey was carried out the week after the occurrence of the tsunami. During the campaign, 24 inundation heights were measured distributed across the flooded area (Fig. 2). These measures combined with

10 those published by the National Geology and Mining Service (SERNAGEOMIN, 2015) and the inundation limit allowed us to model the inundation height in the urban area (a total number of 266 points). The map was estimated using the Geostatistical tool in ArcGIS 10.3 and including a 1 m/pixel Digital Elevation Model as an external drift as the flood height is topography dependent. The obtained modelled map (10 m/pixel) presents a RMSE = 0.54. This field-based reconstructed scenario was used to obtain the flood depth value for each assessed building along the affected area, an essential parameter

15 for the vulnerability index calculation.

3.3 Vulnerability index calculation

We first verified that the spatial information integrated in the GIS geodatabase corresponded with the reality. In those cases where it did not, the polygons were manually modified. Information was also added on buildings under construction as well as those destroyed by the 2015 tsunami. The attributes for each polygon were collected during a field campaign. A total of

20 65 out of 1,239 buildings (5.2%) were not accessible and classified as "No access".
From the different methods published for building vulnerability calculation we chose the PTVA as it has been proved to be a dynamic model in the estimation of tsunami vulnerability across different coastal urban centres around the world. The first and second versions of the model were applied in the Gulf of Corinth, Greece (Papathoma and Dominey-Howes, 2003) and Seaside, Oregon, USA (Dominey-Howes et al., 2010) respectively. After improvements to the model, its third version was

25 tested on the coast of New South Wales, Australia (Dall'Osso et al., 2009b) and has been widely used to assess the vulnerability of several coastal localities such as the Aeolian Islands (Italy; Dall'Osso et al., 2010); Figueira da Foz (Portugal; Barros et al., 2013); Setúbal (Portugal; Santos et al., 2014); the south of the Boso Peninsula (Japan; Voulgaris and Murayama, 2014); the southwest Atlantic coast of Spain (Abad et al., 2014); Naples (Italy; Alberico et al., 2015) and Chabahar Bay (Iran; Madani et al., 2016). Lately, a fourth version of the model has been tested at Botany Bay, Sydney

30 (Australia; Dall'Osso et al., 2016).

3.3.1 The PTVA-3 model

The RVI calculation depends on the Structural Vulnerability (SV) and the Vulnerability to Water intrusion (WV) (Fig. 3). WV is calculated by the relation between the number of inundated levels and the total number of levels, while the SV calculation considers the attributes of the building structure (Building Vulnerability; Bv), the building flood depth

35 (Exposure; Ex) and its protection level (Prot) (Fig. 3).
The Bv calculation considers 6 different attributes (Fig. 3; Table 1). The material attribute (m) was modified and adapted to the constructions methods of Northern Chile (Table 2). The Prot calculation includes 4 attributes (Fig. 3; Table 1) while the Exposure parameter (Ex) is classified from the flood depth map values (Table 3).

3.3.2 The PTVA-4 model

In the PTVA-4 model, the RVI calculation depends on the same parameters as in the PTVA-3 model, i.e. SV and WV (Fig. 3). WV is obtained through the same approach as the PTVA-3 but in this model the parameter accounts for buildings with raised ground floor that will only be inundated if the water depth above the terrain level exceeds the elevation of the ground floor. On the other hand, the attribute mo is now included in the parameter Surr (previous Prot) instead of in BV so all the attributes that consider the building surroundings are now in only one parameter (Figure 3; Table 4). The other modified attribute is Shape and Orientation (so) that was renamed as Shape of Building Footprint (sh) and his values are described in Table 4 and Fig. 3. In addition, in this model, as in the PTVA-3 model, the attribute m was modified and adapted to the constructions of northern Chile (Table 2). Finally, the Ex calculation is the ratio between the water depth impacting the building (WD) and the maximum effective water depth in the study area (WD max). After all procedure, Dall'Osso et al. (2016) suggest that for a better displaying of the RVI results in the case of the PTVA-4 model a more sophisticated technique should be used. We used technique based on the Jenks' Natural Breaks Algorithm (Jenks, 1977), obtaining the final scaling for the RVI classification.

3.4 Model validation

The vulnerability results obtained in the PTVA-3 and PTVA-4 models were compared with the real damages caused by the tsunami to validate both models with a real event on the northern coast of Chile. We used the information provided by MINVU, a total of 484 analysis that correspond to a technical evaluation for the residential houses located in the area hit by the tsunami focused on Baquedano (sector 2) in Coquimbo (Fig. 1). This information was integrated in the geodatabase and compare with our RVI results (Table 5). The building damage classification used by MINVU consists of 4 categories that range from minor damage to non-reparable whereas the RVI obtained from the PTVA models involves 5 categories. To facilitate the comparison of both scales, we have unified the high and very high RVI scores. The expected RVI for each building can then be correlated with its degree of damage described after the tsunami impact. In this sense, Dall'Osso et al. (2016) specify that the RVI scores cannot be used to predict which buildings will reach or exceed a given damage state but to relatively compare the expected performance of each building. Therefore, the aim of our comparison is not to provide a damage description to a given RVI score but to verify if the low RVI scores correspond to minor building damages and vice versa.

4 The September 16, 2015 tsunami

The epicentre of the Illapel earthquake (September 16, 2015) was located at 71.741°W and 31.637°S at a depth of 23.3 km (http://www.sismologia.cl), where the rupture velocities reached 1.5-2.0 km/s (Heidarzadeh et al., 2016). The Illapel earthquake occurred between two lower coupling zones (LCZs): a small zone near 32°S, and a larger one in the north, near 30.5°S in front of La Serena. This seismic event occurred near the northern end of the rupture zone of the 1730 megaearthquake with magnitude Mw ~ 9.0 that probably controls the seismic cycle of central Chile (Ruiz et al., 2016). Considering two earthquakes of magnitude Mw ~8.0 that occurred previously (1943 and 1880; Beck et al., 1998), Nishenko (1985) suggested that the Illapel zone was a seismic gap.

Because of the inter-plate event, a transoceanic tsunami of moderate height was generated, causing damages along the Chilean coasts, especially in the Coquimbo Region. Aránguiz et al. (2016) indicates the tsunami run-up varied between 4 and 6 m in places close to the origin region, even with maximum of 10.8 m. Moreover, local bathymetry and topography promoted the tsunami to cause greater damage in some urbanized coastal locations. The tide gauge record shows that the earthquake occurred shortly after the low tide at the epicentre (Fig. 2a), which means that the highest observed wave of the

tsunami arrived during high tide. The arrival time at Coquimbo was 23 minutes after the earthquake, with 1.1 m of tsunami amplitude. The maximum tsunami amplitude (4.68 m) was measured with the fourth wave.

The Coquimbo Region was the most affected by the tsunami. Authors such as Tomita et al. (2016) indicates that the tsunami was diffracted and refracted by the Coquimbo Peninsula, and then converges to the inner southwestern corner of Coquimbo

5 Bay, located behind the peninsula. In the bay, the maximum vertical run up was 14 m in the Baquedano sector (Fig. 1) whereas towards the north the run up only reaches <0.5 m and according to our reconstruction, the waves penetrated inland more than 950 m in the Elqui mouth and almost 700 m in Culebrón stream mouth, while in Coquimbo port and Serena they only reached 100-200 m and ca. 30 m respectively (Fig. 2b and 2c).

Both the earthquake and the tsunami caused 11 fatalities, 12 injuries while 1 person remain missing and a total of 118,812

10 people affected in Coquimbo Region (CCT-ONEMI, 2015). The most significant effects are recorded in the denominated "Zero Zone" located in the sector of Baquedano and Coquimbo Port. In this place, the tsunami hit hard affecting the port structure, the local market, the fishing creek, commerce and large number of private homes and 17 boats were dragging from the sea. After the tsunami event, MINVU generated a cadastre where 1,921 houses are included with non-repairable damages and 5,364 houses resulted with various types of damages.

5 Vulnerability assessment

5.1 Sector 1 –Coquimbo Port

Coquimbo Port is in the southwestern sector of the Coquimbo Bay (Fig. 1 and 5). The analysis of this sector considers 136 buildings that represent 10.98% of the total flood scenario that reaches here flood depths higher than 2 m (Fig. 2 and 4a). Although it does not present a natural barrier, the buildings in this sector (mostly 1 and 2 stories) are protected by a 3 – 5 m

20 height vertical seawall.

Very high or high RVI occur along the coastline and represent the most important category in the PTVA-4 model (33.83%) while they only represent 23.53% in the PTVA-3 model (Fig. 5 and Table 6). In this first building row, both the waves and movable objects available in the port would impact the buildings (as it happened in 2016; Fig. 4b), which are mainly constructed with light materials (Fig. 4a). On the other hand, some isolated constructions are moderately vulnerable to a

25 tsunami impact, regardless their distance from the coast, due to attributes such as the construction material, the preservation status or the foundations (Fig. 5).

For flood depths ranging from 1 to 2 m, the PTVA-3 model results vary according to the location of the buildings. Most of builds located in second or third row get moderate or average vulnerability when compare with constructions in the first row that score high or average RVI. For PTVA-4 model, a high-moderate RVI is predominant in these flood depths interval.

30 However, in both models, the buildings with minor RVI are affected by flood depths smaller than 1 m. Finally, our results indicate that the model PTVA-4 obtains the largest number of buildings with High and Very high RVI scores (Table 6).

5.2 Sector 2 – Baquedano

Sector 2, located south in the Coquimbo Bay, is partially protected by a small marshland (Fig. 1 and 6) that has been included in the model as a natural barrier (nb=0.5). On the other hand, the non-existence of a seawall in the area together

35 with the low topographic elevation cause that the tsunami floods this area with depths up to 4 m (Fig. 6) affecting a total of 475 buildings (38.34%) (Table 6).

Baquedano is the historical centre of Coquimbo and its residential houses are more than 100 years old. The sector presents a wide variety of building materials from grey block masonry to tin plate, red brick or adobe. First row buildings present RVI scores ranging from minor to very high as the southern ones are protected by marshes bodies that retain the energy

40 propagated by the tsunami wave. In addition, some building features included in the Bv parameter, such as the number of

stories and the foundations, help to decrease the RVI scores. Although partially protected by a marshland, the area is exposed to flood depths > 3 m that result in a very high and high RVI score percentage (7.78% and 11.15% for the PTVA-3 and PTVA-4 models respectively) (Table 6). The most vulnerable buildings in the sector are one or two stories high (Fig. 4c, 4d and 4e) and they are located in the first three building rows. In most cases, buildings with an average or minor RVI

5   correspond to different types of buildings with flood depths < 1m, moderately protected by natural or anthropogenic barriers and/ or reinforced concrete story buildings with more than 5 floors and deep foundations (Fig. 4f), regardless of their location with respect to the coastline (Fig. 6). Most of the buildings (63.16 %) obtain an average RVI score using the PTVA-4 model whereas using the PTVA-3 model only 30.53 % obtained this classification. In the later, most of the buildings are classified as moderate vulnerability (Fig. 6).

10   **5.3 Sector 3 –La Cantera**

La Cantera, located southeast of the Coquimbo Bay (Fig. 1 and 7) presents, as Sector 2 did, a moderate extension of marshland, i.e. a natural barrier, and no seawall protection, with an overall low topographic elevation. The flood scenario shows water depths that range from 0 to 3 m although in the urbanized area depths only reach up to 2 m. Most of the constructions in the sector are detached or bungalow houses isolated and separated several hundred of meters one from

15   another. This circumstance increases the potential damage of the tsunami and movable objects impacts and therefore their vulnerability (Fig. 4g).

A total of 125 buildings have been considered in the sector (10.09% of the total analysis; Table 6). For both PTVA models, buildings with flood depths ranging from 1 to 2 m due to their characteristics (small number of stories, poor ground floor hydrodynamics and/or average depth foundation) and the effect to direct exposure to the tsunami waves and movable objects

20   obtain an average RVI score. On the other hand, most of the buildings with flood depths < 1 m obtained RVI scores that range from minor to moderate using both models. In summary, in this sector the flood area reaches 350 m inland and most of the affected polygons present a moderate RVI (Table 6) however, the PTVA-3 model indicates an average - moderate RVI (83.2%) whereas the PTVA-4 model shows a moderate – minor RVI classification (73.6%) (Fig. 7).

25   **5.4 Sector 4 – Caleta Peñuelas**

Caleta Peñuelas location, between Coquimbo and La Serena, results in almost all its urbanized area affected by the tsunami flood (Fig. 1 and 8). This sector analysis contemplates 26.31% of the total evaluated buildings (326 buildings) (Table 6). In this area, most of the houses are one or two-story buildings (322 houses / 98.77% of buildings total) and according to the tsunami scenario they would be affected by flood depths <1m. In addition, the buildings are generally constructed using

30   lightweight materials such as wood, aluminium or simple brick, with average or shallow foundations. The ground floor hydrodynamics can be generally described as not open plan (Fig. 4h), what causes the building structure to directly receive the tsunami wave. The polygons located between the road and the Pacific Ocean (Fig. 8) are directly constructed in the beach and correspond to restaurants and other facilities that results in average RVI scores in both models mainly due to the low flood depths. Landward, the main group of buildings shows a predominant moderate and minor RVI scores for the PTVA-3

35   and 4 respectively (Table 6).

5.5 Sector 5 – La Pampa

The coastal border of La Pampa is one of the residential and touristic sectors in La Serena (Fig. 1) that according to the reconstructed scenario is very little affected. The flood depths in the sector are < 1m and constrain to a narrow area next to the coastline. The urban development in this sector is mainly characterized by reinforced concrete story buildings with more

40   than 5 floors and deep foundations (23.02 %). The other buildings features are quite heterogeneous including different

construction materials, shallower foundations, and less floors being then, more vulnerable. A total of 120 buildings have been analysed in this sector (9.68% of the total). The results obtained (Fig. 9) classify the area as a relatively safe sector under the 2015 tsunami scenario, with most of the obtained RVI scores being minor in both models (Table 6). This last model obtains the largest number of minor RVI score as most of the polygons correspond to more than 5 stories buildings.

5 **5.6 Sector 6 – La Serena**

The last sector, La Serena, considers 4.6% of the studied polygons, i.e. 57 (Table 6). The flood depth in this area is <1 m with the smallest affected area. As in Sector 5, buildings in La Serena correspond to reinforced concrete structures with more than 5 floors. The RVI assessment shows that La Serena, is a sector with moderate - minor RVI scores for this tsunami scenario (89.48% and 98.25% for the PTVA-3 and PTVA-4 models, respectively) (Table 6). These circumstances are

10 associated with the flood depth in the sector but mainly with the type of constructions (Fig. 10).

6 PTVA-3 vs. PTVA-4 results

The distribution of the final RVI scores in the cities of La Serena – Coquimbo allow us comparing the vulnerability assessment. Fig. 11a shows the distribution of the flood depth impacting each building according to the field-based reconstructed scenario. The maximum value is 3.49 m however, most of the buildings were flooded less than 0.5 m.

15 Dall'Osso et al. (2016) exposed that the Ex, Bv, Prot parameters are better distributed using the PTVA-4 model than with the PTVA-3 due to the difference in the re-scaling procedure adopted by the models. Therefore, according to them the newest model RVI scores should be more representative. Fig. 11b shows the distribution of the final RVI scores obtained with the PTVA-3 and PTVA-4 models. To compare both models we used for the PTVA-4 model the Jenks' Natural Breaks Algorithm (Jenks, 1977) classifying the RVI scores in 5 categories. For the very high and high RVI, both models show a

20 similar number of buildings although the total number in these categories is small and only represents < 10% of the total analysed buildings. The less vulnerable categories do not show a clear tendency. While the number of buildings with minor and average RVI scores in the PTVA-4 is higher this pattern is inverted for the moderate category. In this sense, according to the PTVA-4 model RVI results, the largest number of buildings will be classified as minor and average vulnerability what should be a better reflection of the expected scenario then the PTVA-3 model results (Dall'Osso et al., 2016).

25 **7 Tsunami vulnerability model validation**

As pointed out by Dall'Osso et al. (2016) the PTVA-3 and PTVA-4 models provide a RVI score that can be used to compare the expected performance of buildings. We have compared the two models results with the real damages occurred after the 16S event, which was used for the flood scenario, in Sector 2 (Fig. 12). This sector has its own architectonical characteristics (see 5.2) and was flooded with high flood depths and therefore, it is not representative for the whole study area.

30 Nevertheless, it can be used as a good example to check both models as it presents different flood depths and RVI scores in all the categories. After the tsunami, MINVU assessed a total of 190 buildings in this sector what represents only 40% of the tsunami building vulnerability assessment for the sector in this study (Table 6).
We have compared the RVI trends with the MINVU data trend (Fig. 12), the curves show a unimodal distribution with the maximum located at range 3 in the PTVA models and in range 2 in the actual damages. The latter presents dispersed values

35 along the range-axis without any of the categories being more significant than the others. On the other hand, the PTVA-3 RVI values distribution reveals a normal distribution with a better-defined maximum and a negative asymmetry resulting in smaller RVI scores. Finally, the RVI scores obtained in PTVA-4 show a well-defined peak that is, most of the values are concentrated in one range. Although PTVA-4 model shows better accuracy according to Dall'Osso et al., (2016), our data

suggest a larger imbalance in the trend respect to the PTVA-3 model when compare to the actual performance of buildings trend. In any case, clear differences exist among both models and the real damages in the scenario.

8. Conclusions

This paper analyses and validates the use of the two latest versions of the PTVA model (PTVA-3 and PTVA-4) in a real case
5   scenario, the 16S 2015 event in the cities of La Serena and Coquimbo. Results of both PTVA-3 and PTVA-4 models show that in the scenario the most vulnerable areas are sectors 1 and 2 (Coquimbo Port and Baquedano) what agrees with the most damaged areas after the 2015 tsunami. Both models result in a similar number of very high and high RVI scores although these categories only represent <10% of the total analysed buildings whereas the less vulnerable categories do not show a similar trend and PTVA.4 model obtains a larger number of minor and average RVI scores that should be a better reflection
10   of the expected buildings performance. However, when compare with the actual damages occurred after the 2015 tsunami in the Baquedano sector, the PTVA-3 RVI scores show a normal distribution that is more similar to the actual damages distribution trend than that obtained by the PTVA-4 model that shows a more concentrated distribution of the RVI scores. Even though the Chilean construction regulation is severe, historical buildings are still vulnerable to tsunami impacts and therefore, future tsunami mitigation measures should focus on these areas.

Acknowledgements

15

References

Abad, M., Izquierdo, T., and Ruiz, F.: El registro de tsunamis como herramienta para el análisis y mitigación del riesgo en la costa de Huelva (SO de España), Fundación MAPFRE, Huelva, España, 46 pp., 2014.

20   Alberico, I., Di Fiore, V., Iavarone, R., Petrosino, P., Piemontese, L., Tarallo, D., Punzo, M., and Marsella, E.: The Tsunami Vulnerability Assessment of Urban Environments through Freely Available Datasets: The Case Study of Napoli City (Southern Italy), J. Mar. Sci. Eng., 3, 981-1005, doi:10.3390/jmse3030981, 2015.

Aránguiz, R., González, G., González, J., Catalán, P. A., Cienfuegos, R., Yagi, Y., Okuwaki, R., Urra, L., Contreras, K., Del Rio, I., and Rojas, C.: The 16 September 2015 Chile Tsunami from the Post-Tsunami Survey and Numerical Modeling

25   Perspectives, Pure Appl. Geophys., 173, 333-348, doi:10.1007/s00024-015-1225-4, 2016.

Aránguiz, R., Urra, L., Okuwaki, Y., and Yagi, Y.: Tsunami fragility curve using field data and numerical simulations of the 2015 tsunami in Coquimbo, Chile, Nat. Hazards Earth Syst. Sci., 1-22, doi: 10.5194/nhess-2017-364, under review.

Barros, L., Emídio, A., Tavares, A. O., and Santos, Â.: Metodologias de avaliação da vulnerabilidade ao risco de tsunami: aplicação ao sector costeiro Cova Gala – Leirosa; Figueira da Foz, in: IX Congresso da Geografia Portuguesa, Évora,

30   Portugal, 28-3 Novembro 2013, 839-845, 2013.

Beck, S., Barrientos, S., Kausel, E., and Reyes, M.: Source characteristics of historic earthquakes along the central Chile subduction zone, J. South Am. Earth Sci., 11, 115-129, doi:10.1016/S0895-9811(98)00005-4, 1998.

Bobillier, C.: Año de 1922: Terremoto de Atacama, Boletín del Servicio Sismológico de Chile – XVI, Santiago, Chile, 44 pp., 1926.

35   CCT-ONEMI: Análisis Multisectorial Eventos 2015: Evento Hidrometeorológico Marzo – Terremoto/Tsunami Septiembre, ONEMI, Chile, 56 pp., 2015.

Natural Hazards
and Earth System
Sciences
Discussions

Open Access

Cisternas, M., Atwater, B. F., Torrejón, F., Sawai, Y., Machuca, G., Lagos, M., Eipert, A., Youlton, C., Salgado, I., Kamataki, T., Shishikura, M., Rajendran, C. P., Malik, J. K., Rizal, Y., and Husni, M.: Predecessors of the giant 1960 Chile earthquake, Nature, 437, 404-407, doi:10.1038/nature03943, 2005.

Cisternas, M., Garrett, E., Wesson, R., Dura, T., and Ely, L. L.: Unusual geologic evidence of coeval seismic shaking and tsunamis shows variability in earthquake size and recurrence in the area of the giant 1960 Chile earthquake, Mar. Geol., 385, 101-113, doi: 10.1016/j.margeo.2016.12.007, 2017.

Contreras-López, M., Winckler, P., Sepúlveda, I., Andaur-Álvarez, A., Cortés-Molina, F., Guerrero, C. J., Mizobe, C. E., Igualt, F., Breuer, W., Beyá, J. F., Vergara, H., and Figueroa-Sterquel, R.: Field Survey of the 2015 Chile Tsunami with Emphasis on Coastal Wetland and Conservation Areas, Pure Appl. Geophys., 173, 349-367, doi:10.1007/s00024-015-1235-2, 2016.

Dall'Osso, F., Gonella, M., Gabbianelli, G., Withycombe, G., and Dominey-Howes, D.: A revised (PTVA) model for assessing the vulnerability of buildings to tsunami damage, Nat. Hazards Earth Syst. Sci., 9, 1557–1565, doi:10.5194/nhess-9-1557-2009, 2009a.

Dall'Osso, F., Gonella, M., Gabbianelli, G., Withycombe, G., and Dominey-Howes, D.: Assessing the vulnerability of buildings to tsunami in Sydney, Nat. Hazards Earth Syst. Sci., 9, 2015-2026, doi:10.5194/nhess-9-2015-2026, 2009b.

Dall'Osso, F., Maramai, A., Graziani, L., Brizuela, B., Cavalletti, A., Gonella, M., and Tinti, S.: Applying and validating the PTVA-3 Model at the Aeolian Islands, Italy: assessment of the Vulnerability of buildings to tsunamis, Nat. Hazards Earth Syst. Sci., 10, 1547-1562, doi:10.5194/nhess-10-1547-2010, 2010.

Dall'Osso, F., Dominey-Howes, D., Tarbotton, C., Summerhayes, S., and Withycombe, G.: Revision and improvement of the PTVA-3 model for assessing tsunami building vulnerability using ''international expert judgment'': introducing the PTVA-4 model, Nat. Hazards, 83, 1229-1256, doi:10.1007/s11069-016-2387-9, 2016.

DeMets, C., Gordon, R. G., and Argus, D. F.: Geologically current plate motions, Geophys. J. Int., 181, 1-80, doi:10.1111/j.1365-246X.2009.04491.x, 2010.

Dominey-Howes, D., Dunbar, P., Varner, J., and Papathoma-Köhle, M.: Estimating probable maximum loss from a Cascadia tsunami, Nat. Hazards, 53, 43-61, doi:10.1007/s11069-009-9409-9, 2010.

Dunbar, P., McCullough, H., Mungov, G., Varner, J., and Stroker, K.: Tohoku earthquake and tsunami data available from the National Oceanic and Atmospheric Administration/National Geophysical Data Center, Geomat Nat Haz Risk, 2, 305-323, doi:10.1080/19475705.2011.632443, 2011.

Ely, L. L., Cisternas, M., Wesson, R. L., Dura, T.: Five centuries of tsunamis and land-level changes in the overlapping rupture area of the 1960 and 2010 Chilean earthquakes, Geology, 42, 995-998, doi:10.1130/G35830.1, 2014.

Fuentes, M., Riquelme, S., Hayes, G., Medina, M., Melgar, D., Vargas, G., González, J., and Villalobos, A.: A Study of the 2015 Mw 8.3 Illapel Earthquake and Tsunami: Numerical and Analytical Approaches, Pure Appl. Geophys., 173, 1847-1858, doi:10.1007/s00024-016-1305-0, 2016.

Hidalgo, R., Arenas, F., and Monsalve R.: La conurbación La Serena – Coquimbo: problemas y desafíos de su transformación metropolitana, Chile: del país urbano al país metropolitano, Hidalgo, R., de Mattos, C. A., and Arenas, F., Pontificia Universidad Católica de Chile, Santiago, Chile, 161-184, 2009.

Jenks, G. F.: Optimal data classification for choropleth maps, Occasional Paper No. 2, Department of Geography, University of Kansas, Kansas, USA, 1977.

Jordan, T. E., Isacks, B. L., Allmendinger, R. W., Brewer, J. A., Ramos, V. A., and Ando, C. J.: Andean tectonics related to geometry of subducted Nazca plate, Geol. Soc. Am. Bull., 94, 341-361, doi:10.1130/0016-7606(1983)94<341:ATRTGO>2.0.CO;2, 1983.

Kempf, P., Moernaut, J., Van Daele, M., Vandoorne, W., Pino, M., Urrutia, R., and De Batist, M.: Coastal lake sediments reveal 5500 years of tsunami history in south central Chile, Quat. Sci. Rev., 161, 99-116, doi:10.1016/j.quascirev.2017.02.018, 2017.

Kulikov, E. A., Rabinovich, A. B., and Thomson, R. E.: Estimation of Tsunami Risk for the Coasts of Peru and Northern Chile, Nat. Hazards, 35, 185-209, doi:10.1007/s11069-004-4809-3, 2005.

Lomnitz, C.: Major Earthquakes of Chile: A Historical Survey, 1535-1960, Seismol. Res. Lett., 75, 368-378, doi:10.1785/gssrl.75.3.368, 2004.

Lunecke, M. G. H.: Planificación territorial y mitigación de impacto de tsunami en Chile después del 27 Febrero 2010, Revista de Urbanismo, 0, 20-33, 2016.

Madani, S., Khaleghi, S., Jannat, M. R. A.: Assessing building vulnerability to tsunami using the PTVA-3 model: A case study of Chabahar Bay, Iran, Nat. Hazards, 85, 349-359, doi:10.1007/s11069-016-2567-7, 2016.

Maureira, G. C.: Estudio del impacto turístico-inmobiliario en el borde costero de Coquimbo y La Serena, Chile, Revista Turismo em Análise, 9, 88-106, doi:10.11606/issn.1984-4867.v9i2p88-106, 1998.

McBride, O. A. G., Zamora, D. M. M., and Page, F. M. T.: De ciudad mediterránea a metrópolis costera: El caso de gran La Serena, Revista Urbano, 19, 30-43, 2016.

Nishenko, S. P.: Seismic potential for large and great interpolate earthquakes along the Chilean and southern Peruvian margins of South America: A quantitative reappraisal, J. Geophys. Res., 90, 3589–3615, doi:10.1029/JB090iB05p03589, 1985.

Papathoma, M. and Dominey-Howes, D.: Tsunami vulnerability assessment and its implications for coastal hazard analysis and disaster management planning, Gulf of Corinth, Greece, Nat. Hazards Earth Syst. Sci., 3, 733-747, doi:10.5194/nhess-3-733-2003, 2003.

Pardo, M., Comte, D., and Monfret, T.: Seismotectonic and stress distribution in the central Chile subduction zone, J. South Am. Earth Sci., 15, 11-22, doi:10.1016/S0895-9811(02)00003-2, 2002.

Ruiz, S., Klein, E., del Campo, F., Rivera, E., Poli, P., Metois, M., Christophe, V., Baez, J. C., Vargas, G., Leyton, G., Madariaga, R., and Fleitout, L.: The Seismic Sequence of the 16 September 2015 Mw 8.3 Illapel, Chile, Earthquake, Seismol. Res. Lett., 87, 1-11, doi:10.1785/0220150281, 2016.

Santos, A., Tavares, A. O., and Emidio, A.: Comparative tsunami vulnerability assessment of an urban area: An analysis of Setúbal city, Portugal, Appl. Geogr., 55, 19-29, doi: 10.1016/j.apgeog.2014.08.009, 2014.

SERNAGEOMIN: Zonas afectadas por inundación por Tsunami Comuna de Coquimbo. Mapa de inundación del 21 de septiembre de 2015. 2015.

Simons, M., Minson, S. E., Sladen, A., Ortega, F., Jiang, J., Owen, S. E., Meng, L., Ampuero, J., Wei, S., Chu, R., Helmberger, D. V., Kanamori, H., Hetland, E., Moore, A. W., and Webb, F. H.: The 2011 Magnitude 9.0 Tohoku-Oki Earthquake: Mosaicing the Megathrust from Seconds to Centuries, Science, 332, 1421-1425, doi:10.1126/science.1206731, 2011.

SHOA: El Maremoto del 22 de Mayo de 1960 en las costas de Chile, 2, SHOA, Valparaíso, Chile, 72 pp., 2000.

SHOA: Registro de los principales tsunamis que han afectado a la costa de Chile, available at: http://www.shoa.cl/servicios/tsunami/data/tsunamis_historico.pdf, 2016.

Smith, R.: The biggest one, Nature, 465, 24-25, doi:10.1038/465024a, 2010.

Soloviev, S. L., and Go, C. N.: Catalogue of Tsunamis on the Eastern Shore of the Pacific Ocean, Nauka Publ. House, Moscow, 204 pp., 1975. (in Russian; English translation: Canadian Transl. Fish. Aquatic Sci., Ottawa, 5078, 293 pp., 1984).

Tassara, A., Götze, H. J., Schmidt, S., and Hackney, R.: Three-dimensional density model of the Nazca plate and the Andean continental margin, J. Geophys. Res., 111, B9, doi:10.1029/2005JB003976, 2006.

Tomita, T., Arikawa, T., Takagawa, T., Honda, K., Chida, Y., Sase, K., and Olivares, R. A. O.: Results of Post-Field Survey
on the Mw 8.3 Illapel Earthquake Tsunami in 2015, Coast. Eng. J., 58, 1-17, doi:10.1142/S05785635416500030, 2016.

Voulgaris, G. and Murayama, Y.: Tsunami Vulnerability assessment in the Southern Boso Peninsula, Japan, Int. J. Disaster
Risk Reduct., 10, 190-200, doi:10.1016/j.ijdrr.2014.09.001, 2014.

5

Table 1. Attributes and their values influencing the structural vulnerability of a building (Bv) and its level of protection (Prot) in PTVA-3 model (Dall'Osso et al., 2009a).

	-1	-0,5	0	+0,25	+0,5	+0,75	+1
s	> 5 stories	4 stories	3 stories		2 stories		1 story
g	Open plan	Open plan and windows	50% open plan		Not open plan, but many windows		Not open plan
f	Deep pile foundation		Average depth foundation				Shallow foundation
so	Poor hydrodynamic shape		Average hydrodynamic shape				High hydrodynamic shape
mo			Minimum risk of being damaged by movable objects	Moderate risk of being damaged by movable objects	Average risk of being damaged by movable objects	High risk of being damaged by movable objects	Extreme risk of being damaged by movable objects
pc	Excellent	Good	Average		Poor		Very poor
Prot_br			>10th	7-8-9-10th	4-5-6th	2nd-3rd	1st
Prot_nb			Very high protection	High protection	Average protection	Moderate protection	No protection
Prot_sw			Vertical and >5m	Vertical and 3 to 5m	Vertical and 1.5 to 3m	Vertical and 0 to 1.5m or sloped and 1.5 to 3m	Sloped and 0 to 1.5m or no seawall
Prot_w			Height of the wall is from 80% to 100% of the water depth	Height of the wall is from 60% to 80% of the water depth	Height of the wall is from 40% to 60% of the water depth	Height of the wall is from 20% to 40% of the water depth	Height of the wall is from 0% to 20% of the water depth

5

Table 2. Original parameter (m) (Dall'Osso et al., 2009a) and modified according to the constructions of northern Chile.

	-1	-0,5	0	+0,25	+0,5	+0,75	+1
m (original)	Reinforced concrete		Double brick		Single brick		Wood
m (modified)	Reinforced concrete	Gray block	Red brick		Adobe		Wood and / or metal

5

10

Table 3. Numeric values assigned to the Ex parameter.

16S Flood Depth (m.a.s.l)	Ex
0-1	1
1-2	2
2-3	3
3-4	4

Natural Hazards
and Earth System
Sciences
Open Access
Discussions
EGU

Table 4. Attributes and their values influencing the structural vulnerability of a building (Bv) and its surroundings characteristics

(Surr) in PTVA-4 model (Dall'Osso et al., 2016).

	-1	-0,5	0	+0,5	+1
s	More than 5 stories	4 stories	3 stories	2 stories	1 story
g	Completely open plan (e.g. no walls, only columns)	About 75 % open plan	About 50 % open plan	About 25 % open plan	Completely closed plan, no or very few openings at ground floor
f	Deep pile foundation		Average depth foundation		Shallow foundation
sh	Round-like or triangular	Squared or almost squared	Rectangular	Lengthened rectangular	Complex (L, T or X shaped buildings, or other complex geometries)
pc	Very good	Good	Average	Poor	Very poor
br	>10th	7-8-9-10th	4-5-6th	2nd-3rd	1st
nb	Very high protection	High protection	Average protection	Moderate protection	No protection
sw	Vertical and >5m	Vertical and 3 to 5m	Vertical and 1.5 to 3m	Vertical and 0 to 1.5m or sloped and 1.5 to 3m	Sloped and 0 to 1.5m or no seawall
w	Height of the wall is from 80% to 100% of the water depth	Height of the wall is from 60% to 80% of the water depth	Height of the wall is from 40% to 60% of the water depth	Height of the wall is from 20% to 40% of the water depth	Height of the wall is from 0% to 20% of the water depth
mo	Very low risk from movable objects		Average risk from movable objects		Very high risk from movable objects

5

Table 5. Established ranges for RVI and actual damage comparison.

Range	RVI	MINVU Damage	Description
1	Minor	Minor repairable	Affected house with nonstructural damages in terminations.
2	Moderate	Moderate repairable	Affected house with moderate damages although still repairable that do not impede the habitability of the house.
3	Average	Major repairable	Affected house with major damages that do not impede the habitability of the house.
4	High and very high	Non-Repairable	Affected house with non-repairable damages that prevent its habitability.
-	No access	Without residents and/or without damage	-

5

Natural Hazards and Earth System Sciences — Open Access — Discussions — EGU

Table 6. Number of analyzed polygon in each sector and the obtained RVI score for PTVA-3 and PTVA-4 models.

| Sector	Scenario	Very high	High	Average	Moderate	Minor	No access	Total
Coquimbo Port	16S_PTVA-3	10 (7.35%)	22 (16.18%)	37 (27.21%)	39 (28.67%)	26 (19.12%)	2 (1.47%)	136
	16S_PTVA-4	7 (5.15%)	39 (28.68%)	58 (42.65%)	10 (7.35%)	20 (14.70)	2 (1.47%)	
Baquedano	16S_PTVA-3	9 (1.89%)	28 (5.89%)	145 (30.53%)	197 (41.47%)	86 (18.11%)	10 (2.11%)	475
	16S_PTVA-4	8 (1.68%)	45 (9.47%)	300 (63.16%)	43 (9.05%)	69 (14.53%)	10 (2.11%)	
La Cantera	16S_PTVA-3	0 0%	0 0%	52 (41.60%)	52 (41.60%)	19 (15.20%)	2 (1.60%)	125
	16S_PTVA-4	0 0%	0 0%	31 (24.80%)	52 (41.60%)	40 (32.00%)	2 (1.60%)	
Caleta Peñuelas	16S_PTVA-3	0 0%	0 0%	59 (18.10%)	137 (42.03%)	82 (25.15%)	48 (14.72%)	326
	16S_PTVA-4	0 0%	0 0%	26 (7.98%)	78 (23.93%)	174 (53.37%)	48 (14.72%)	
La Pampa	16S_PTVA-3	0 0%	0 0%	21 (17.5%)	41 (34.17%)	56 (46.67%)	2 (1.67%)	120
	16S_PTVA-4	0 0%	0 0%	3 (2.5%)	37 (30.83%)	78 (65.00%)	2 (1.67%)	
La Serena	16S_PTVA-3	0 0%	0 0%	5 (8.77%)	38 (66.67%)	13 (22.81%)	1 (1.75%)	57
	16S_PTVA-4	0 0%	0 0%	0 0%	15 (26.32%)	41 (71.93%)	1 (1.75%)	
Total	16S_PTVA-3	19 (1.53%)	50 (4.04%)	319 (25.75%)	504 (40.68%)	282 (22.76%)	65 (5.25%)	1,239
	16S_PTVA-4	15 (1.21%)	84 (6.78%)	418 (33.74%)	235 (18.97%)	422 (34.06%)	65 (5.25%)	

5
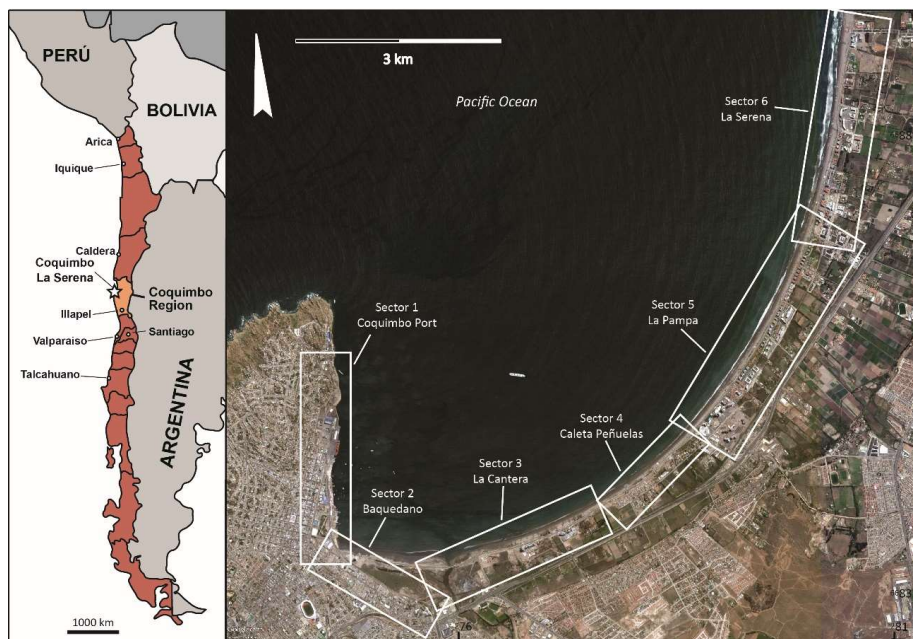
Figure 1: Location of the study area and the analysed sectors in the Coquimbo Bay (image courtesy of Google Earth).
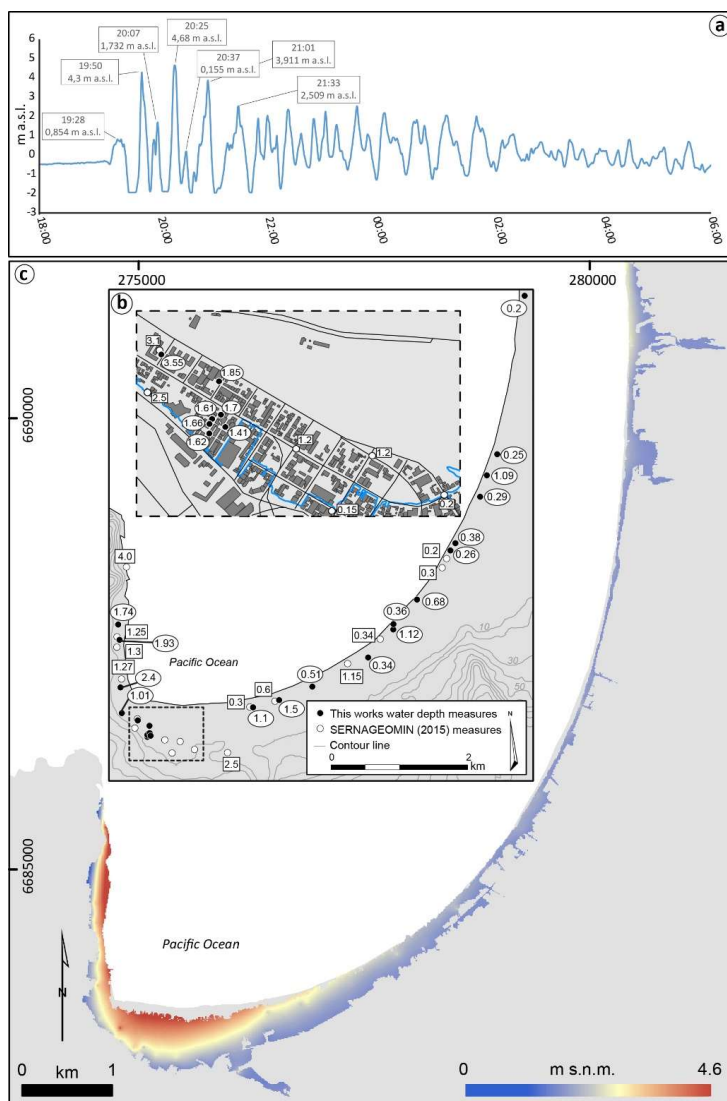
Figure 2: a) Coquimbo tide gauge measurements (SHOA); b) Flood depth measurements along Coquimbo and La Serena; the blue line marks the limit of the flood;c) reconstructed tsunami inundation map and flood depths from the data collected in the field.
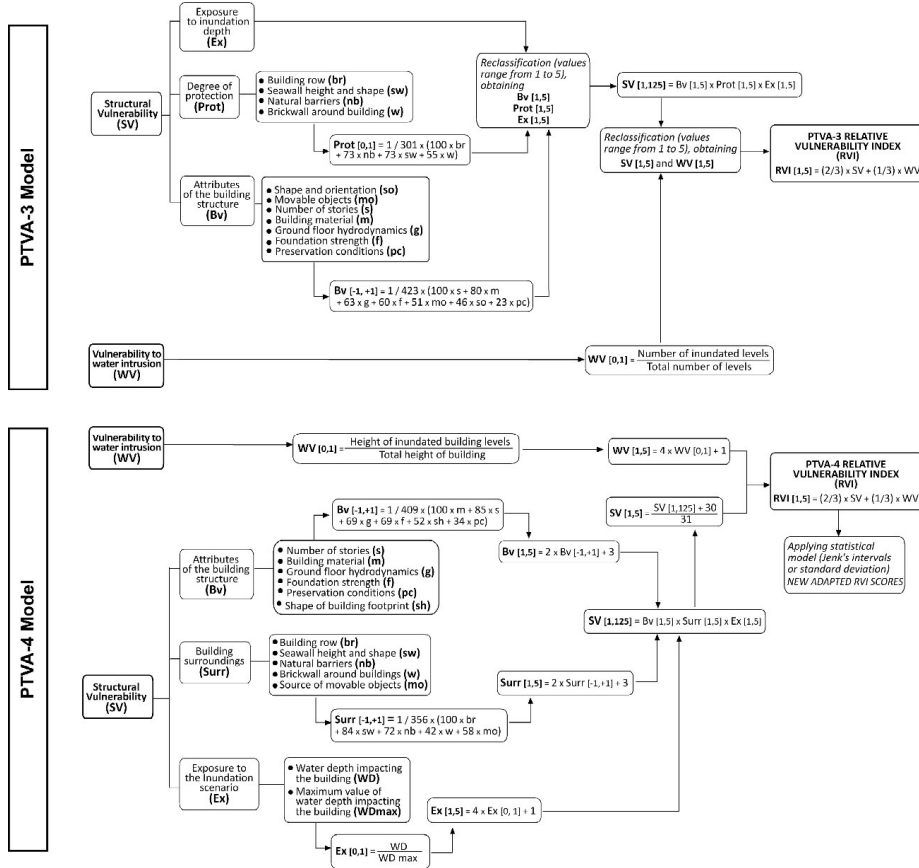
5

Natural Hazards
and Earth System
Sciences
Discussions
Open Access

EGU

Figure 3: PTVA-3 and PTVA-4 models.

Natural Hazards
and Earth System
Sciences

Discussions

Figure 4: a) Building with average RVI score in the first coastline with flood heights of 1.9 m after the 2015 tsunami in Coquimbo Port (sector 1); b) Movable objects impacting residential buildings after the 2015 tsunami; c) High vulnerability building with more than 50% of its infrastructure flooded; d) High vulnerability building with its damaged infrastructure after the 2015 tsunami; e) Very high vulnerability building that resulted in non-repairable damage after the 2015 tsunami; f) Modern buildings with minor vulnerability RVI score; g) Very high vulnerability building highly affected by the tsunami in La Cantera sector; h) Not open plan ground floor.
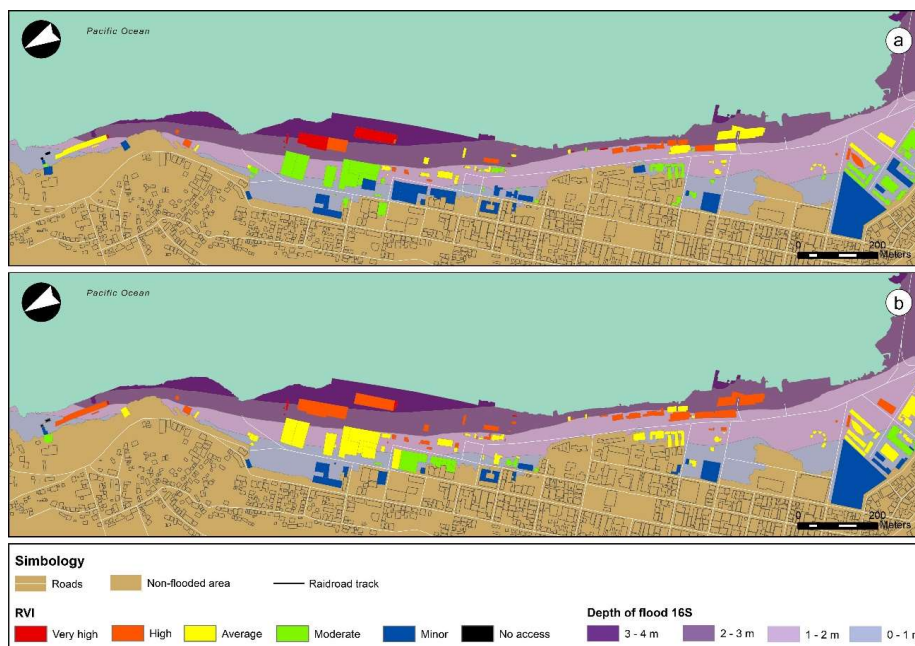
Figure 5: Relative Vulnerability Index for Sector 1 - Coquimbo Port: a) PTVA-3 model; b) PTVA-4 model.
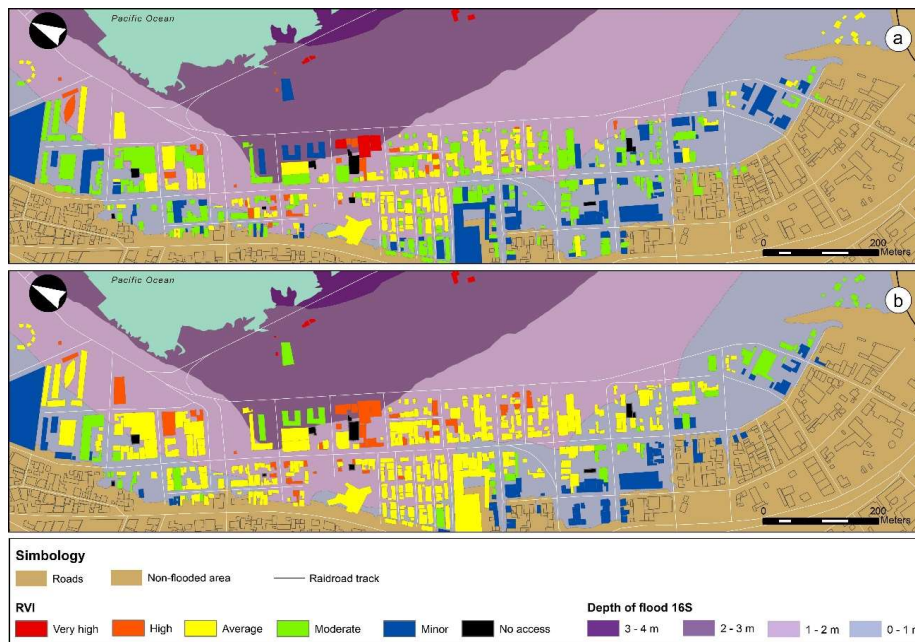
Figure 6: Relative Vulnerability Index for Sector 2 - Baquedano: a) PTVA-3 model; and d) PTVA-4 model.
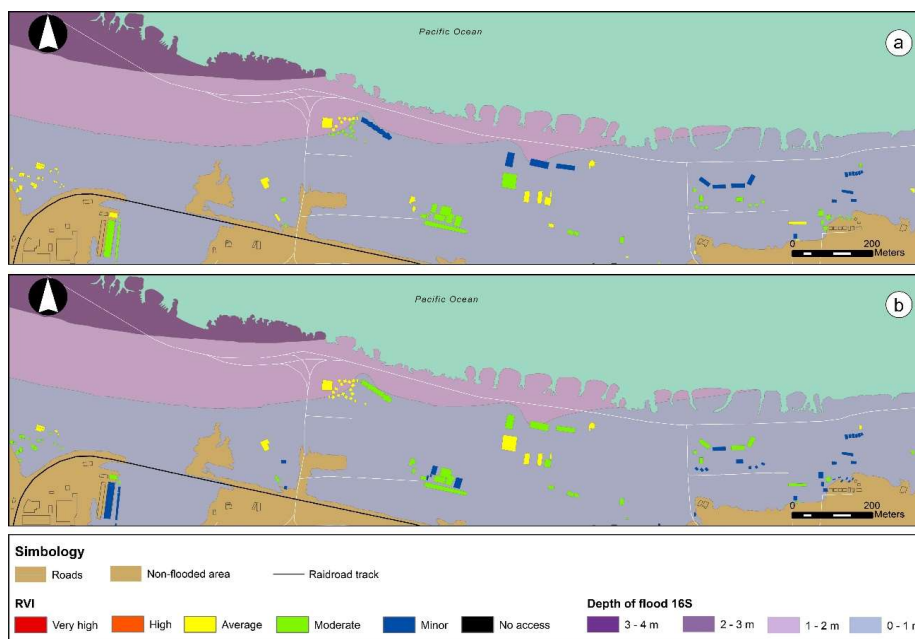
Figure 7: Relative Vulnerability Index for Sector 3 - La Cantera: a) PTVA-3 model; and d) PTVA-4 model.
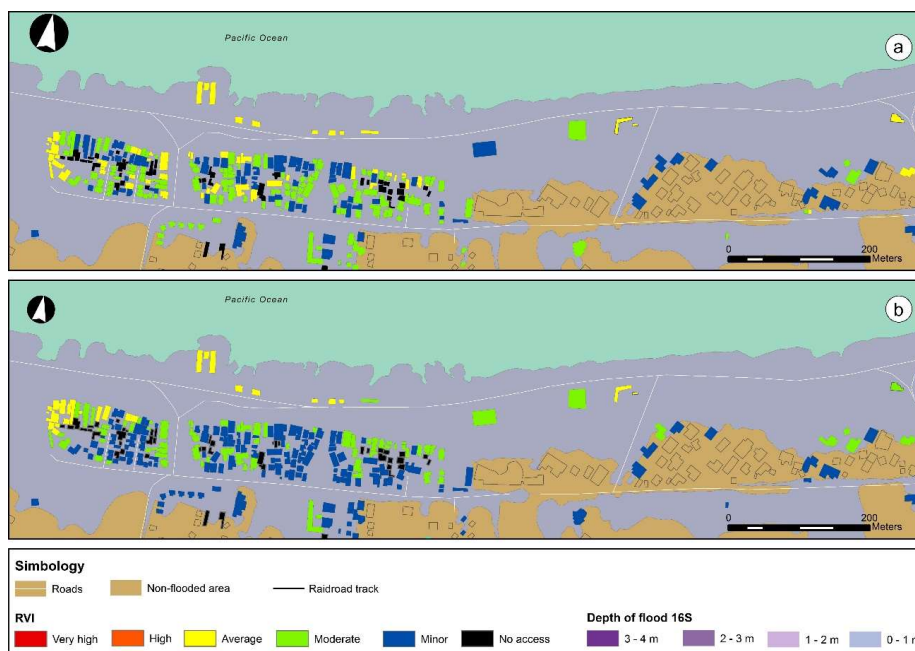
Figure 8: Relative Vulnerability Index for Sector 4 - Caleta Peñuelas: a) PTVA-3 model; and d) PTVA-4 model.

Figure 9: Relative Vulnerability Index for Sector 5 - La Pampa: a) PTVA-3 model; and d) PTVA-4 model.

Figure 10: Relative Vulnerability Index for Sector 6 - La Serena: a) PTVA-3 model; and d) PTVA-4 model.

Natural Hazards
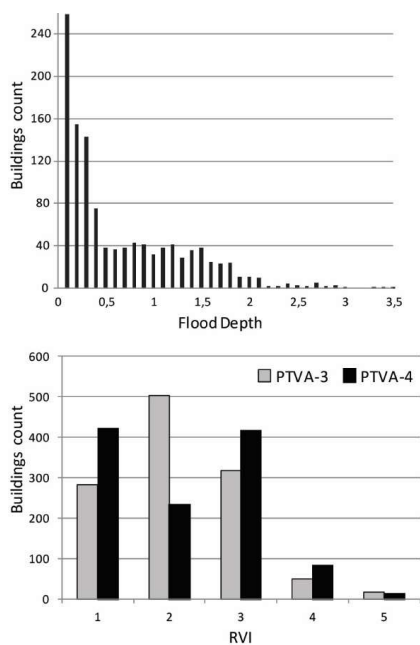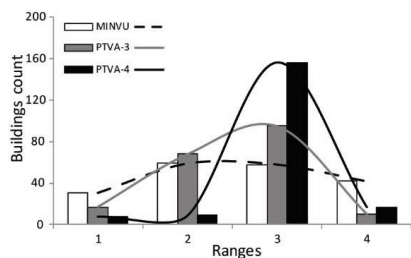and Earth System
Sciences
Discussions

Figure 11: a) Number of buildings exposed to the different water depth (WD) ranges in Coquimbo Bay in the reconstructed 2015 tsunami scenario; b) RVI scores obtained for the total 1,239 buildings analyzed after the PTVA-3 and PTVA-4 models.

5

10

Figure 12: Number of buildings in the different established ranges.